



ENHANCED RESERVOIR CHARACTERIZATION OF PHEM FIELD, OFFSHORE NIGER DELTA: INTEGRATION OF SEISMIC ATTRIBUTES AND RESERVOIR PROPERTY MODELING

Rotimi SALAMI¹ , Adeolu O. ADEPETUN¹ 

¹ Olusegun Agagu University of Science and Technology (OAUSTECH), School of Earth Sciences, Department of Applied Geophysics, Okitipupa, Ondo State, Nigeria

E-mail: salamrotimi@yahoo.com

ABSTRACT

This study provides a comprehensive characterization of hydrocarbon-bearing reservoirs in the Phem Field, offshore Niger Delta, integrating well logs, seismic attributes, and petrophysical modeling for enhanced exploration and production. Three key reservoirs (R-1, R-2, and R-3) were identified within the Agbada Formation, exhibiting intercalated sand and shale layers with variable thickness and significant hydrocarbon potential. Well log analyses based on gamma ray (GR), resistivity, and neutron-density (N-D) logs revealed increasing shale content with depth, aligning with the stratigraphy of the Agbada Formation. Time and depth structure maps highlighted key structural features and hydrocarbon trapping mechanisms, supported by fault-controlled anticlinal structures. Seismic attribute analysis, particularly RMS amplitude and average envelope, delineated high-amplitude zones correlating with high-porosity sands and favorable reservoir facies, providing strategic targets for exploration. Petrophysical modeling, including net-to-gross (NTG), porosity, and permeability models, confirmed superior reservoir quality in specific zones, with NTG values reaching 95% and porosity ranging from 0.12 to 0.42. Additionally, water and hydrocarbon saturation models underscored zones with strong hydrocarbon presence and minimal water content, marking promising areas for efficient hydrocarbon recovery. These integrated findings highlight the Phem Field's robust hydrocarbon potential, offering valuable insights for optimized reservoir management and future development.

Keywords: Agbada Formation; Niger Delta; Petrophysical Modeling; Reservoir Characterization; Seismic Attributes.

1 INTRODUCTION

Enhanced reservoir characterization is a pivotal area of focus in the oil and gas industry, aiming to improve portfolio performance and optimize resource extraction [9], [13]. Accurate reservoir characterization leads to higher success rates and reduces the number of wells required for effective exploitation [5]. In this study, we address the need for advanced interpretation techniques by integrating seismic attributes and 3D reservoir modeling for the Phem-Field, offshore Niger Delta. Reservoir characterization involves the comprehensive study of reservoir properties through geologic, geophysical, petrophysical, and engineering disciplines [6]. This process includes understanding geometric features such as structural and stratigraphic controls, depositional facies, and petrophysical properties like porosity, fluid saturation, and permeability. The goal is to construct a predictive model using various data types, employing both descriptive and quantitative methods [25], [8].

The integration of 3D seismic data plays a crucial role in this endeavor. Seismic data is utilized for structural mapping, detailed stratigraphic interpretations, and reservoir descriptions, providing essential inputs for geologic modeling [28], [7]. Techniques such as seismic inversion, attribute analysis, and spectral decomposition are instrumental in predicting

reservoir properties and their dynamic behavior [39], [9]. Seismic attributes, particularly those derived from 3D seismic data, are valuable for reservoir characterization. These attributes help predict reservoir properties and monitor their changes over time. Selecting appropriate attributes is critical to accurately describing relevant reservoir properties and avoiding spurious correlations [28], [13], [5]. This study aims to enhance the reservoir characterization of Phem-Field by integrating seismic attributes with 3D geological modeling. The objectives include delineating lithologies, identifying hydrocarbon-bearing reservoirs, conducting seismic structural interpretation, analyzing seismic attributes for hydrocarbon prospectivity, building a representative 3D geological model, and providing future recommendations.

Reservoir heterogeneities, which vary from pore scale to major reservoir units, significantly impact reservoir properties and performance predictions. Addressing these heterogeneities through robust qualitative and quantitative approaches is essential for accurate reservoir modeling and optimal hydrocarbon recovery [26], [6]. By leveraging both well-log and seismic data, this study aims to construct a detailed geomodel of Phem-Field, capturing the key heterogeneities and enhancing reservoir connectivity and performance predictions. In summary, this research seeks to improve reservoir characterization techniques by integrating seismic attributes with 3D reservoir modeling, ultimately contributing to more effective resource management and extraction strategies in the Phem-Field, offshore Niger Delta.

2 LOCATION OF STUDY AREA AND GEOLOGY

The Phem field, located within the offshore depobelt of the Niger Delta Basin in Nigeria, is positioned at 05°01'11" N latitude and 04°88'51" E longitude (Fig. 1). This field is part of an active oil operation in the Gulf of Guinea, within the broader Niger Delta province [20]. Since the Eocene, the delta has expanded southwestward, forming large depobelts that represent its most active developmental stages [11]. These depobelts, among the world's largest, span 300,000 km² with sediment volumes reaching 500,000 km³ and thicknesses exceeding 10 km at the basin's center [21], [17], [19].

The Niger Delta is underpinned by the Tertiary Akata-Agbada petroleum system, influenced by tectonic structures tied to the South Atlantic's opening [11]. Situated in the southwestern part of the Benue Trough, the basin is bordered by the Cameroon Volcanic Line and a passive continental margin. The basin evolved from an extensional rift system, which began in the late Jurassic, producing faults and syn-rift sands and shales. Post-rift, a Paleocene transgression led to further sediment deposition, shaping the basin's three main formations:

- **Benin Formation:** Predominantly non-marine sands from alluvial settings, accumulating since the Oligocene.
- **Agbada Formation:** Comprising hydrocarbon-rich sands, silts, and clays deposited cyclically from the Eocene, with a thickness over 3,700 meters.
- **Akata Formation:** Marine shales with turbidite sands, formed from the Paleocene, acting as both source rocks and potential reservoirs.

The basin's tectonic framework consists of extensional, transitional, and contractional zones, driven by Cretaceous fracture zones along the West African coast [23]. Gravity-induced deformation and shale mobility became dominant after rifting ceased in the Late Cretaceous, creating a clastic sequence up to 12,000 meters thick. The delta developed through multiple depositional cycles from the early Cretaceous to the Cenozoic, shaped by balanced sedimentation and subsidence. Depobelts, ranging from 30 to 60 km wide, prograde southwest over oceanic crust, influenced by synsedimentary faulting and sediment supply variations [11]. Each depobelt shows distinct structural features, reflecting the internal gravity tectonics of the delta.

The basin petroleum system

The Niger Delta basin's petroleum system centers on the Agbada Formation, which holds most hydrocarbon reserves. An "oil-rich belt" extends northwest to southeast offshore, aligned with the continental-oceanic crust transition where sediment thickness peaks. Petroleum generation began in the Eocene and continues, with migration mainly through faults. Structural traps like rollover structures, antithetic faults, and clay-filled channels are common, while stratigraphic traps are significant along the delta margins [11]. The interbedded shales within the Agbada Formation

act as effective seals. Source rocks in the Akata Formation have sufficient organic content, though maturity varies. Reservoir rocks from the Eocene to Pliocene offer good porosity and permeability, often forming stacked bodies. Petroleum migration is driven by episodic expulsion from over-pressured shales, similar to the Gulf of Mexico system [18].

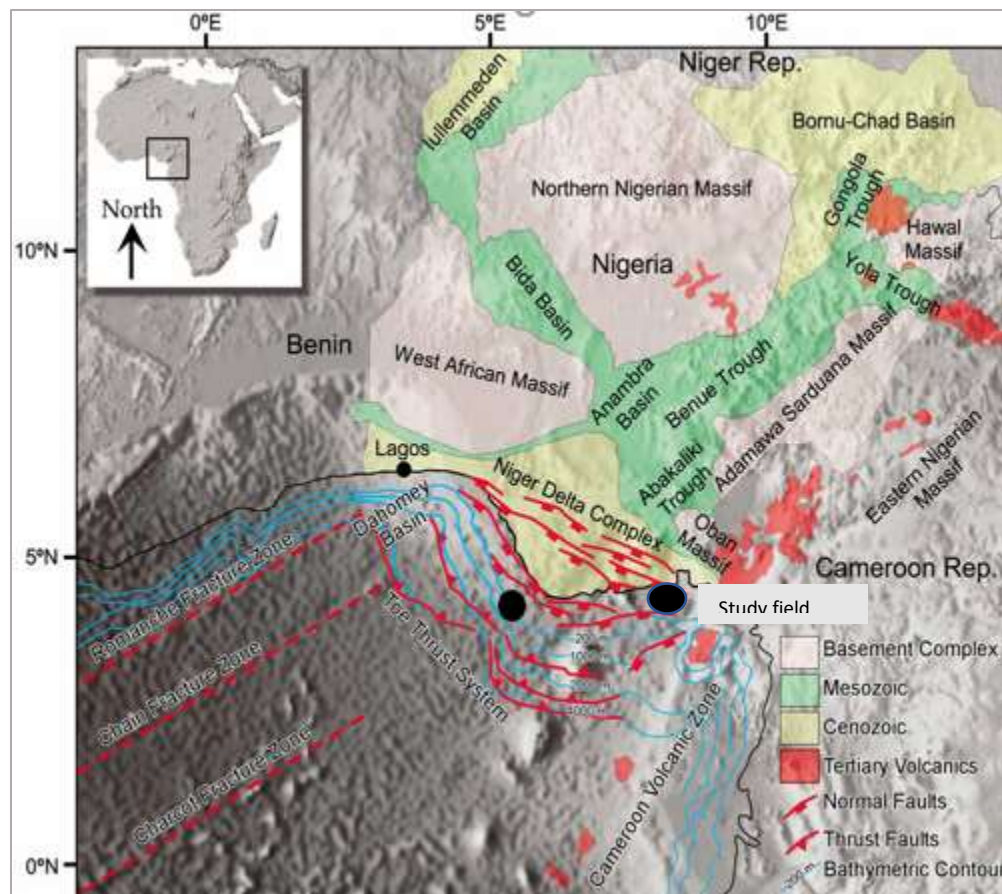


Figure 1. Map showing the location of PHEM Field within the offshore depobelt of the Niger Delta Basin. The field is positioned at latitude $05^{\circ}01'11''$ N and longitude $04^{\circ}88'51''$ E, marking its strategic location within an active hydrocarbon exploration area in the Niger Delta (modified after [14])

3 DATA SET AND METHODOLOGY

Seismic data and a suite of well logs were collected from the Niger Delta Basin's offshore depobelt. This dataset includes 3-D seismic data and well logs from five wells (Phem-01 – Phem-05), along with deviation and check shot data, and a base map of the well locations (Fig. 2). Petrel software was used for interpreting seismic and well logs, with check shot data available only for wells Phem-01 and Phem-05.

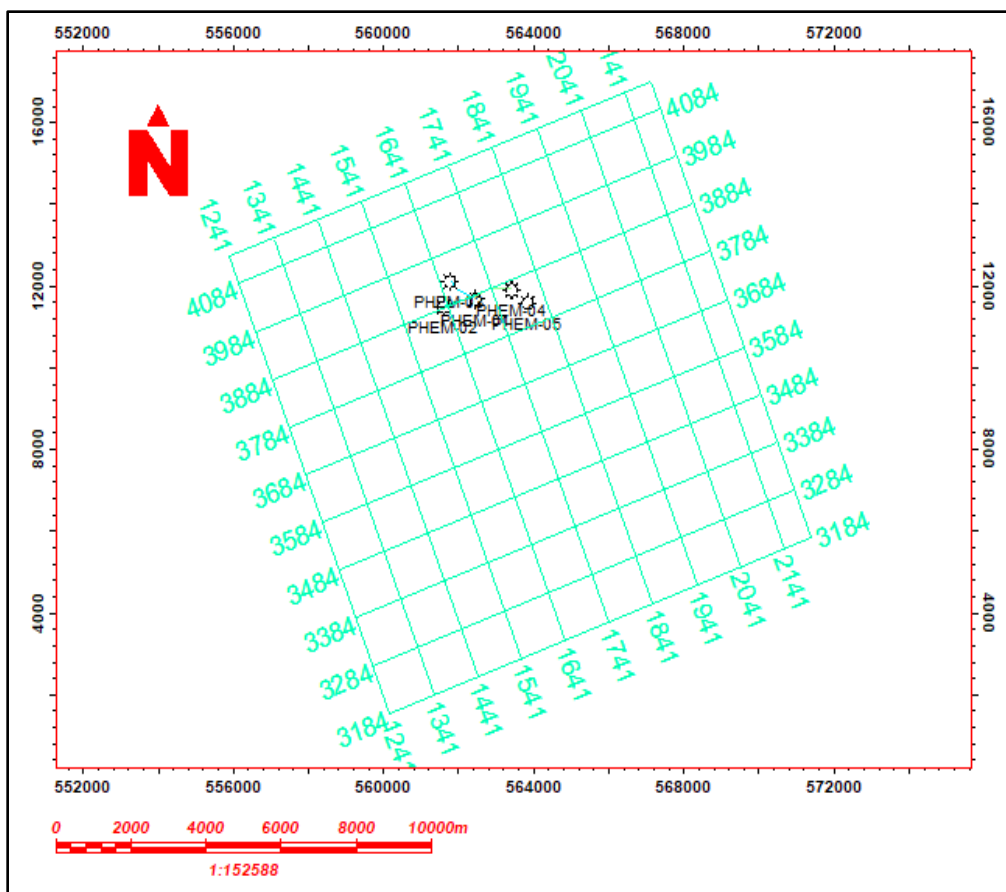


Figure 2 Base map showing the location of wells PHEM-01 – PHEM-05 in the offshore Niger Delta Basin

3.1 Well log analysis

Log analysis is essential in well log interpretation, focusing on identifying geological formations penetrated by the well, particularly hydrocarbon-bearing units. This analysis utilizes gamma ray (GR), density, and deep resistivity logs to distinguish between sand and shale formations [38]. Well logs are measurements obtained via instruments lowered into a borehole during or post-drilling, providing continuous data plotted against depth [41]. These logs are critical for petrophysical analysis and formation evaluation, offering insights into reservoir characteristics such as porosity, permeability, and fluid saturations. Logs can be acquired from LWD (Logging While Drilling) or wireline logging data [38].

3.2 Wells correlation

Wells were correlated to deduce the lateral continuity of delineated reservoirs using electric log correlation techniques [35]. This process involved correlating five wells using gamma-ray and resistivity logs, which are effective for identifying geological continuity and reservoir extents [30]. The GR and resistivity logs are particularly highlighted as valuable tools for well correlation due to their ability to distinguish between different rock types and fluid contents, facilitating accurate reservoir characterization [35].

3.3 Lithological identification

Lithological identification refers to the qualitative interpretation of well log data aimed at recognizing different rock types based on their responses in the logs [36], [30]. In this study, GR log was used to distinguish primary rock types. By establishing a baseline for sand and shale on the log, areas with higher GR responses were identified as shale, while those with lower GR readings were identified as sand [36], [30], [33]. The log's scale ranged from 0 to 150 API, with a central cut-off point at 75 API; values below 75 API indicated sand, whereas values above 75 API indicated shale [36], [30], [32].

3.4 Reservoir and non-reservoir delineation

Reservoir and non-reservoir delineation were achieved using GR and deep resistivity measuring tools [36], [30], [32]. High resistivity and low GR responses typically indicate hydrocarbon-bearing zones, as hydrocarbons exhibit high resistivity. Conversely, low resistivity within sand bodies suggests water-bearing zones. This qualitative approach facilitated the delineation of hydrocarbon-bearing sand intervals, crucial for reservoir characterization and exploration [36], [30], [32].

3.5 Reservoir fluid identification

Reservoir fluid identification relied on resistivity and neutron-density (N-D) crossover techniques [3], [30], [31]. A significant crossover indicates oil presence, while a decrease in density log alongside a decrease in neutron log suggests gas effect [3], [31]. Gas effect, resulting from gas in pore spaces, causes high porosity values in density logs and low porosity values in neutron logs [36].

3.6 Seismic data processing

Well-to-seismic ties integrated well log interpretations with seismic data by creating a synthetic seismogram from acoustic impedance logs convolved with a Butterworth wavelet (Fig. 3). A 4ms time shift ensured alignment between synthetic and field seismograms. Reservoir tops (R-1, R-2, R-3) corresponded to troughs, indicating low impedance sands beneath high impedance shales.

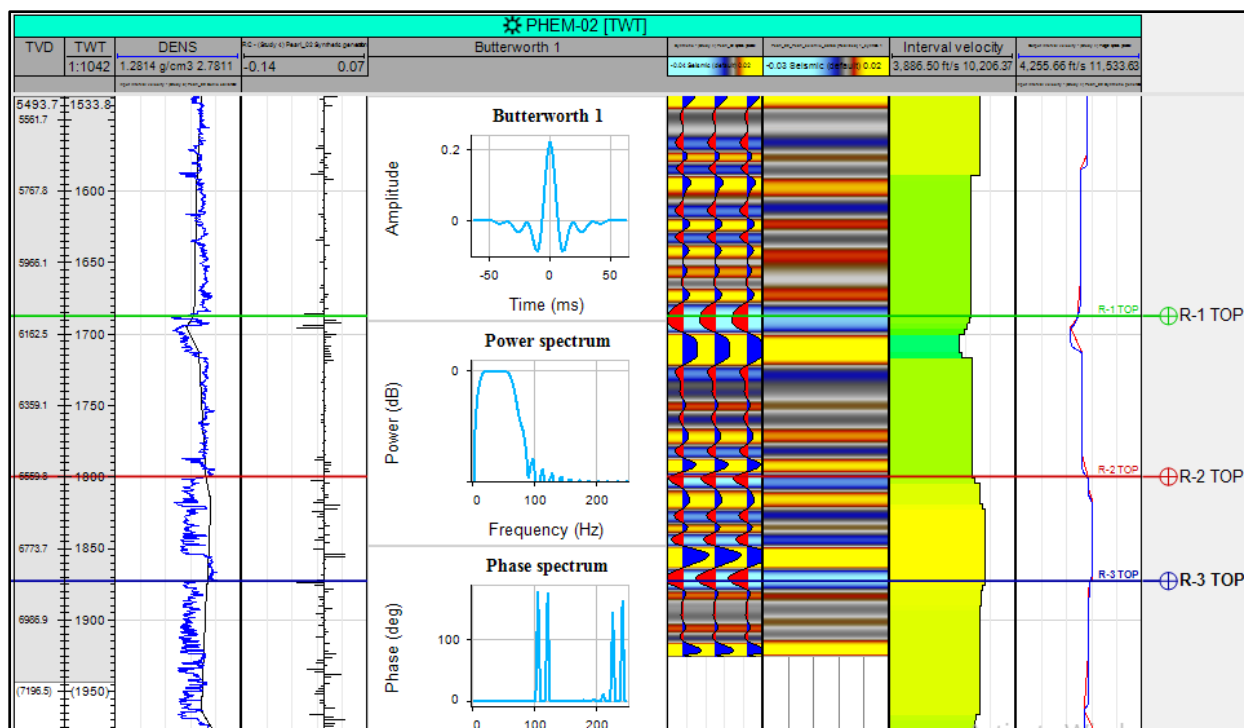


Figure 3. Well-to-seismic tie for PHEM-02 well showing synthetic seismogram alignment and reservoir top correlation

Horizon mapping, essential for subsurface structure understanding, was conducted using Petrel software, enhancing efficiency and accuracy in structural interpretation [40], [6].

3.6.1 Time structural maps

Time-based structural maps were created for mapped horizons using Petrel software, based on two-way travel time data. Advanced contouring techniques, including Convergent Interpolation and Sequential Gaussian simulation, enhanced the precision of structural features by ensuring data continuity and incorporating spatial variability [37]. These contoured maps were linked to well tops, facilitating accurate seismic-to-well correlation. This integration is essential for reliable geological interpretations and constructing subsurface models, aiding exploration and production planning [6], [40].

3.6.2 Time to depth conversion

Time maps were converted to depth using a velocity model developed by the average velocity property method, employing a polynomial function. The primary input for this conversion was the Depth-Time pairs derived from check shot data. This approach enables the creation of a precise velocity model, essential for transforming two-way travel time into accurate depth measurements. The depth conversion is critical for accurate geological and reservoir modeling, providing a realistic representation of subsurface structures and aiding in exploration and production planning [45], [40].

3.6.3 Depth structural maps

These are critical tools in geological and geophysical studies, used to visualize subsurface structures by mapping geological features at various depths below the Earth's surface. These maps are created using data from seismic surveys, well logs, and other geophysical methods, enabling geologists to interpret the spatial distribution of rock layers, faults, and other structural features. The main goal of these maps is to offer a 3-D view of subsurface geology, crucial for hydrocarbon exploration, groundwater management, and tectonic studies [40]. By converting time-based seismic data to depth, these maps offer more accurate representations of geological formations, aiding in the identification of potential resource deposits and guiding drilling operations [45].

3.7 Seismic attributes analysis

Seismic attributes have become vital tools in reservoir characterization, particularly with the advent of 3D seismic data. These attributes, which are quantitative measures extracted from seismic data, can predict reservoir properties and monitor their dynamics [7], [6]. Different attributes provide various types of information, making the selection of appropriate attributes crucial for describing relevant reservoir properties. The advantages of 3D seismic data include extensive spatial coverage and dense sampling, with typical grid spacing around 12.5 by 12.5 meters [28]. This allows for detailed analysis of geological features, such as the size and distribution of sand bodies in deltaic environments. Seismic attributes are extensively used for mapping petrophysical properties and building 3D geological models [13], [12]. However, the quantitative interpretation of seismic data faces challenges like limited vertical resolution and nonuniqueness in the relationship between seismic attributes and geological properties. Attributes may respond to various physical parameters, making it difficult to distinguish between different properties [16]. The danger of spurious correlations – where uncorrelated variables appear related by chance – increases with the number of attributes analyzed. Therefore, careful selection and combination of seismic attributes, alongside geologic knowledge, are necessary to avoid significant errors, such as false positives and false negatives [24].

3.7.1 Root Mean Square (RMS) analysis

Seismic attributes, such as Root Mean Square (RMS) amplitude, are vital in interpreting seismic data for hydrocarbon exploration. RMS amplitude measures the energy of seismic reflections, helping to identify geological features and fluid content in reservoirs [9]. This attribute enhances the visualization of subsurface structures and stratigraphy [42].

3.7.2 Average envelope seismic attribute analysis

The average envelope seismic attribute is crucial for enhancing subsurface imaging by providing insights into the continuity and strength of seismic reflections. This attribute aids in identifying stratigraphic features, lithological variations, and fluid content within reservoirs [8]. By analyzing the amplitude envelope, geophysicists can better delineate geological boundaries and improve reservoir characterization [42].

3.8 3D reservoir model

Reservoir modeling involves constructing a computer model of a petroleum reservoir to improve reserve estimates, guide field development, and predict future production [22]. Geologists and geophysicists create these models to provide a static reservoir description before production. In this study, structural, facies, and petrophysical models were built using available datasets. Zonation and layering refined the grid into smaller units (Fig.4a-d), facilitating property modeling of facies and petrophysical parameters like porosity and permeability [4].

3.8.1 Facies modeling

Facies modeling is essential for representing geological heterogeneity within a reservoir. It involves classifying and distributing rock types based on depositional environments and sedimentary processes, enhancing predictions of reservoir properties and fluid flow behavior [34], [27].

3.8.2 Petrophysical modeling

Petrophysical modeling quantifies reservoir properties such as porosity, permeability, and fluid saturations. This process integrates well log and core data to create spatial distributions of these properties, essential for reservoir simulation and management [43], [44].

3.8.3 Net-to-gross thickness model

The net-to-gross thickness model represents the ratio of reservoir rock to non-reservoir rock within a geological formation. This model is crucial for evaluating reservoir quality and calculating hydrocarbon volumes [15], [27].

3.8.4 Porosity model

Porosity models depict the spatial distribution of void spaces within reservoir rocks, influencing fluid storage and flow. Accurate porosity modeling is vital for estimating hydrocarbon reserves and designing extraction strategies [2], [43].

3.8.5 Permeability model

Permeability models represent the ability of reservoir rocks to transmit fluids. These models are essential for predicting production rates and designing reservoir management strategies [29], [43].

3.8.6 Water saturation model

Water saturation models quantify the proportion of pore space occupied by water in reservoir rocks. These models are critical for evaluating hydrocarbon reserves and designing production strategies [1], [3].

3.8.7 Hydrocarbon saturation model

Hydrocarbon saturation models indicate the fraction of pore space filled with hydrocarbons. These models are crucial for estimating recoverable oil and gas volumes and guiding reservoir development [36], [10].

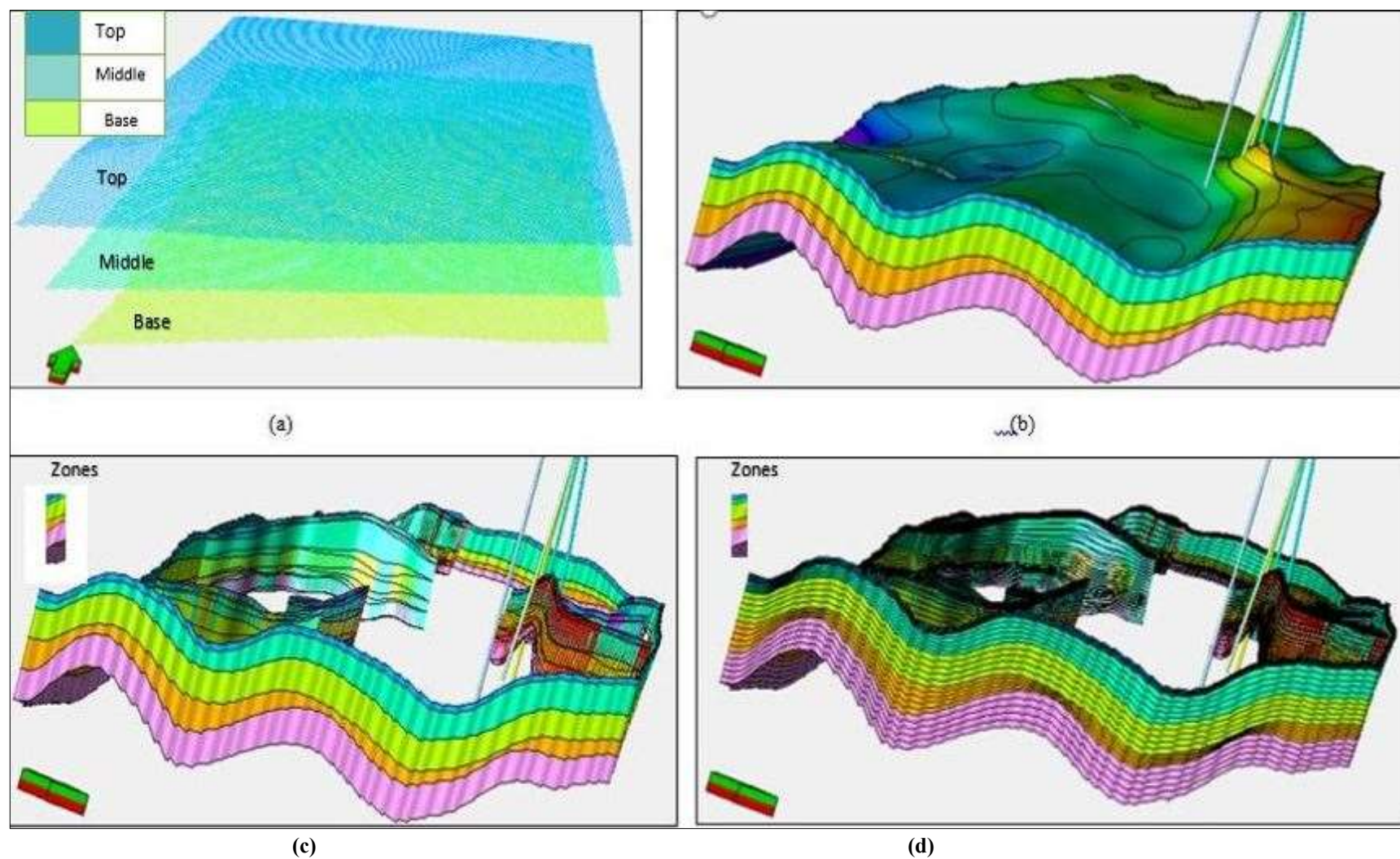


Figure 4. (a) Pillar gridding showing the top, middle, and base; (b) Horizon interpretation of the three reservoirs; (c) Zoning of the three reservoirs in the generated model; (d) Layering of the zones in the generated model

4 RESULTS AND DISCUSSION

4.1 Well log correlation and lithology identification

The well log correlation, based on GR, resistivity, and N-D logs, identified three hydrocarbon-bearing reservoirs (R1, R2, and R3) within the Agbada Formation. The correlation revealed increasing shale and decreasing sand thickness with depth (Fig. 5). Lithologic delineation in the Phem field, using GR and Vsh logs, showed intercalated sand and shale units with a GR cut-off of 75 API. Sand units exhibited low GR values, while shale units had higher values, consistent across wells Phem-01 to Phem-05, reflecting typical Agbada Formation stratigraphy (Fig. 5).

4.2 Reservoir and fluid delineations

Three reservoirs (R-1, R-2, and R-3) were identified based on high resistivity values, indicating potential hydrocarbon presence. The identification was supported by neutron and density logs, displayed on a single track (Fig. 5). These logs collectively enhanced the accuracy of reservoir identification, crucial for hydrocarbon exploration and production strategies.

4.3 Time structure maps of reservoir tops R-1, R-2, and R-3

The time structure maps of the three reservoirs (Fig. 6, 7, and 8) highlight key structural features and hydrocarbon trapping mechanisms. Reservoir R-1 (Fig.6) spans 1640 to 2000 ms, displaying structural highs in the northeastern and southwestern regions. Hydrocarbon entrapment is controlled by anticlinal structures and fault-assisted closures in the northern portion. Reservoir R-2 (Fig.7), ranging from 1760 to 2120 ms, exhibits similar features with structural highs and fault-controlled anticlinal traps. Reservoir R-3 (Fig.8), extending from 1840 to 2200 ms, mirrors trends observed in R-1 and R-2, with anticlinal structures and fault aided hydrocarbon accumulation, particularly in the northern part. The combination of anticlinal structures and faulting across all the reservoirs facilitates hydrocarbon trapping, with wells strategically located in the northern area to exploit these fault-assisted closures.

4.4 Depth structure maps of reservoir tops R-1, R-2, and R-3

The depth structure maps of R-1, R-2, and R-3 (Fig. 9, 10 and 11) closely align with their respective time structure maps, confirming the accuracy of the velocity model used in time-depth conversion. Reservoir R-1(Fig.9.) ranges from 5850 ft. to 7500 ft. with a 40 ft. contour interval. The structural configuration mirrors the time structure map, showing consistent interpretation with structural highs in the northeastern and southwestern areas. Reservoir R-2 (Fig.10) spans 6300 ft. to 7800 ft. and also consistent with the time structure map of R-2. Reservoir R-3 (Fig.11), ranging from 6600 ft. to 8250 ft. with a 40 ft. contour interval, follows a similar pattern, confirming the effective time-depth conversion. The interpretation of structural highs and hydrocarbon trapping mechanisms matches the time structure analysis. Hence, the depth structure maps for all reservoirs maintain consistent structural interpretations, reinforcing the robustness of the velocity model and confirming reliable hydrocarbon trapping mechanisms.

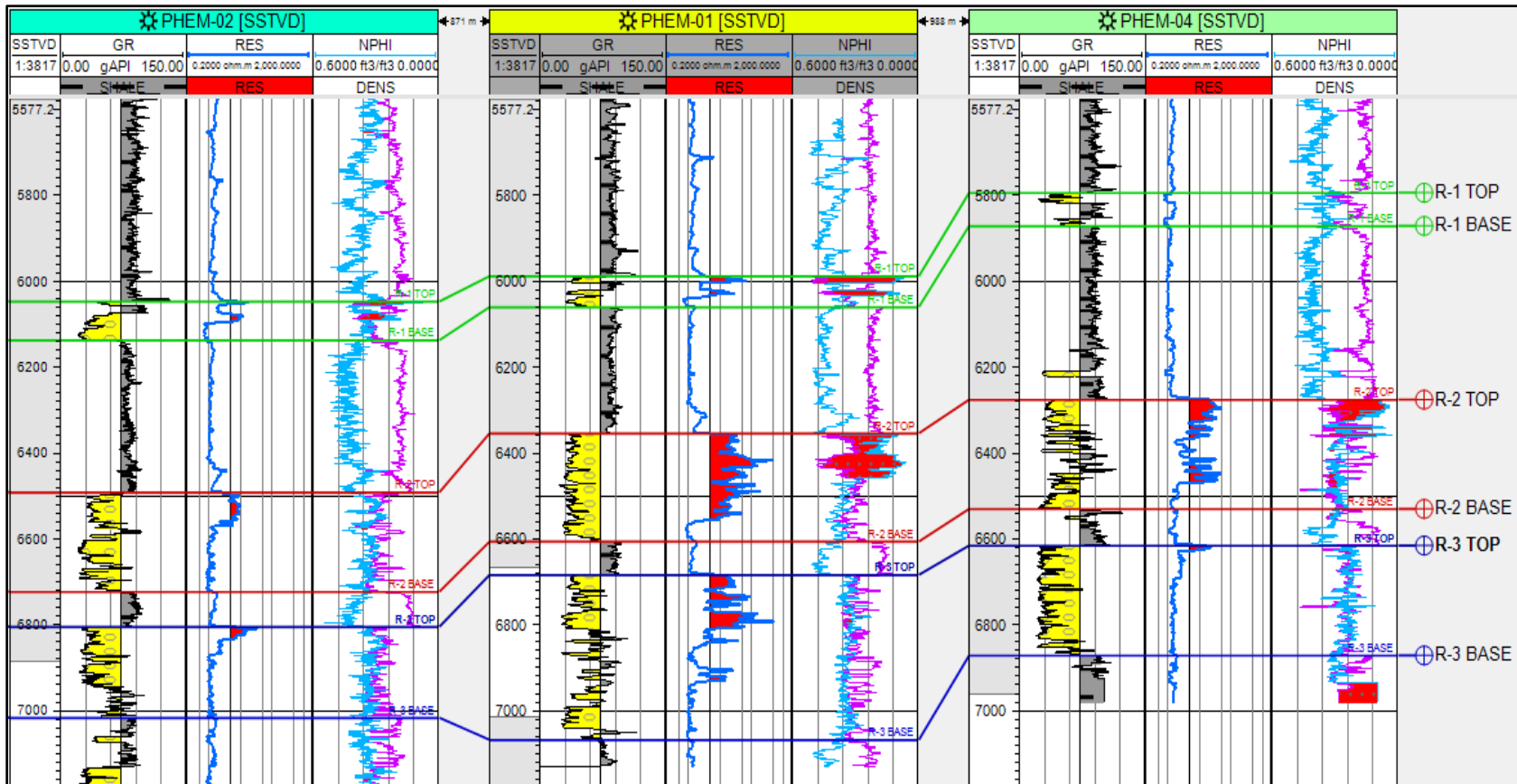


Figure 5. Well log correlation and lithology identification showing hydrocarbon-bearing reservoirs (R1, R2, R3) and intercalation of sand and shale units in the Phem Field

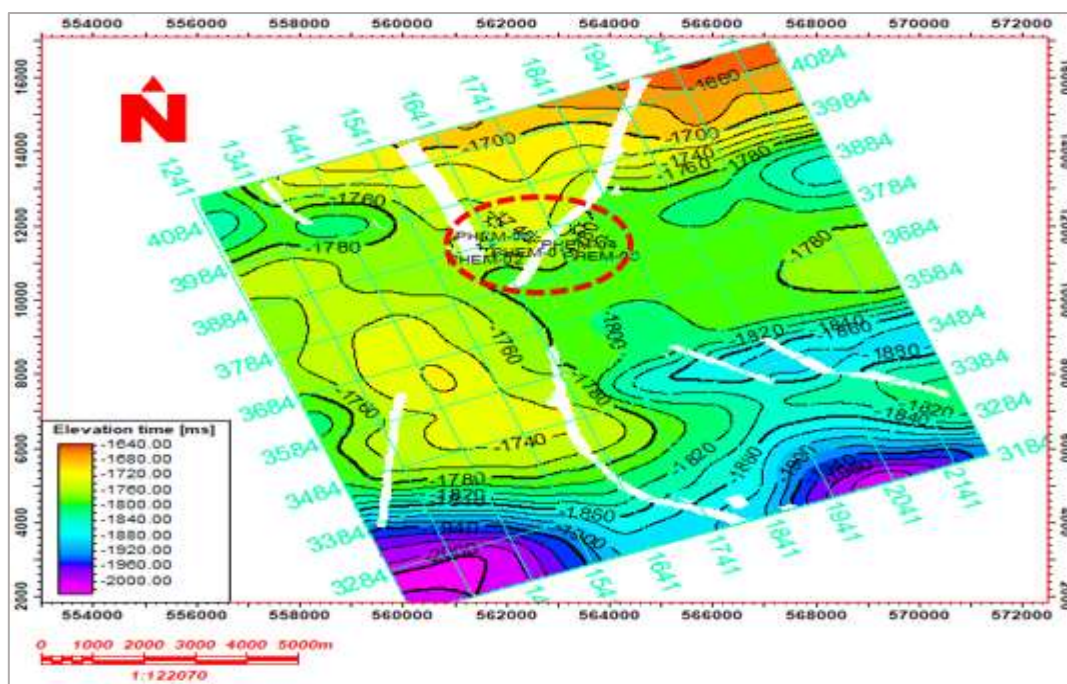


Figure 6. Time Structure Map of Reservoir Top R-1 Highlighting Anticlinal Traps and Fault-Assisted Closures

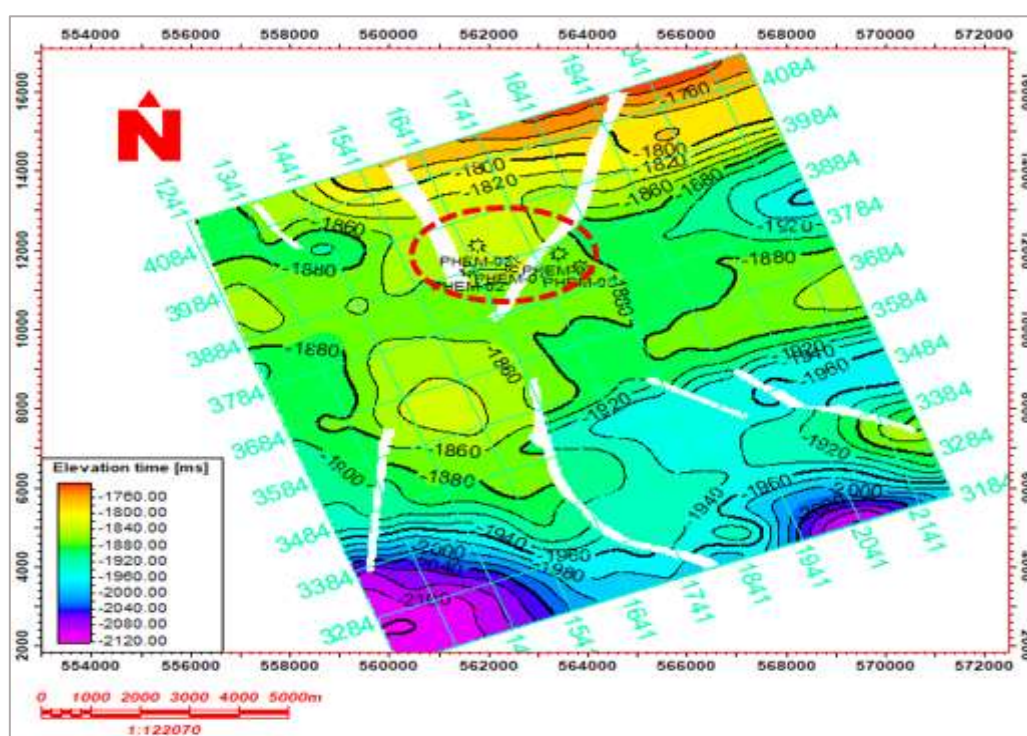


Figure 7. Time structure map of reservoir top R-2 showing structural highs and fault network-influenced hydrocarbon entrapmen

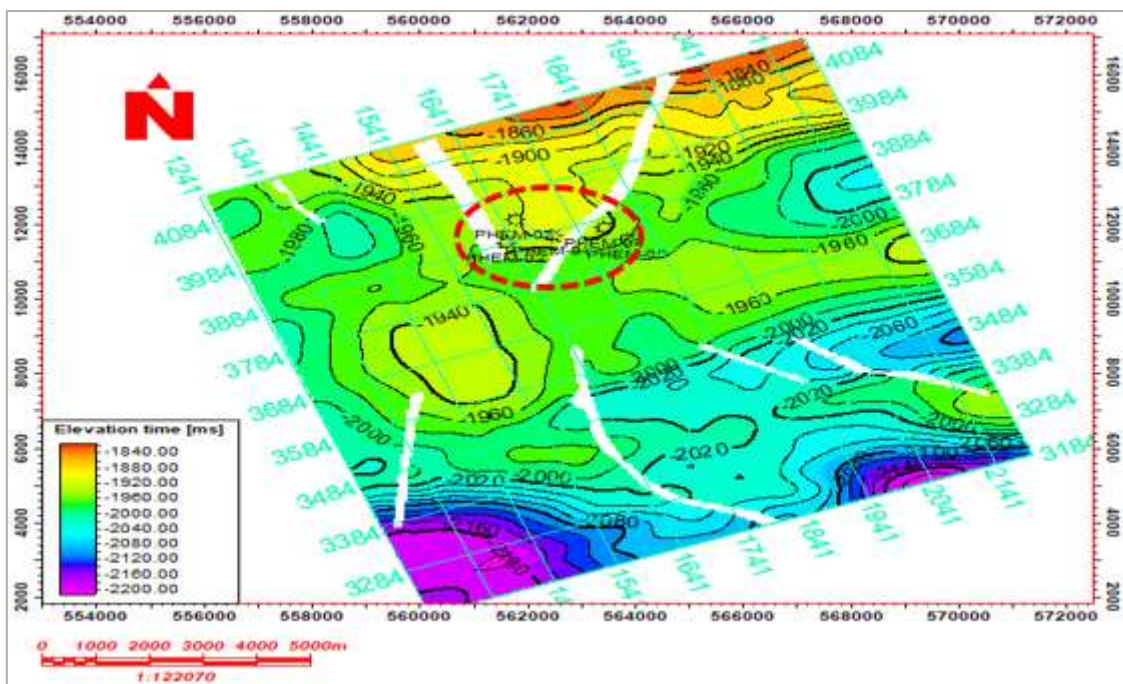


Figure 8. Time structure map of reservoir top R-3 depicting anticlinal structures and strategic well positioning in fault-assisted closures

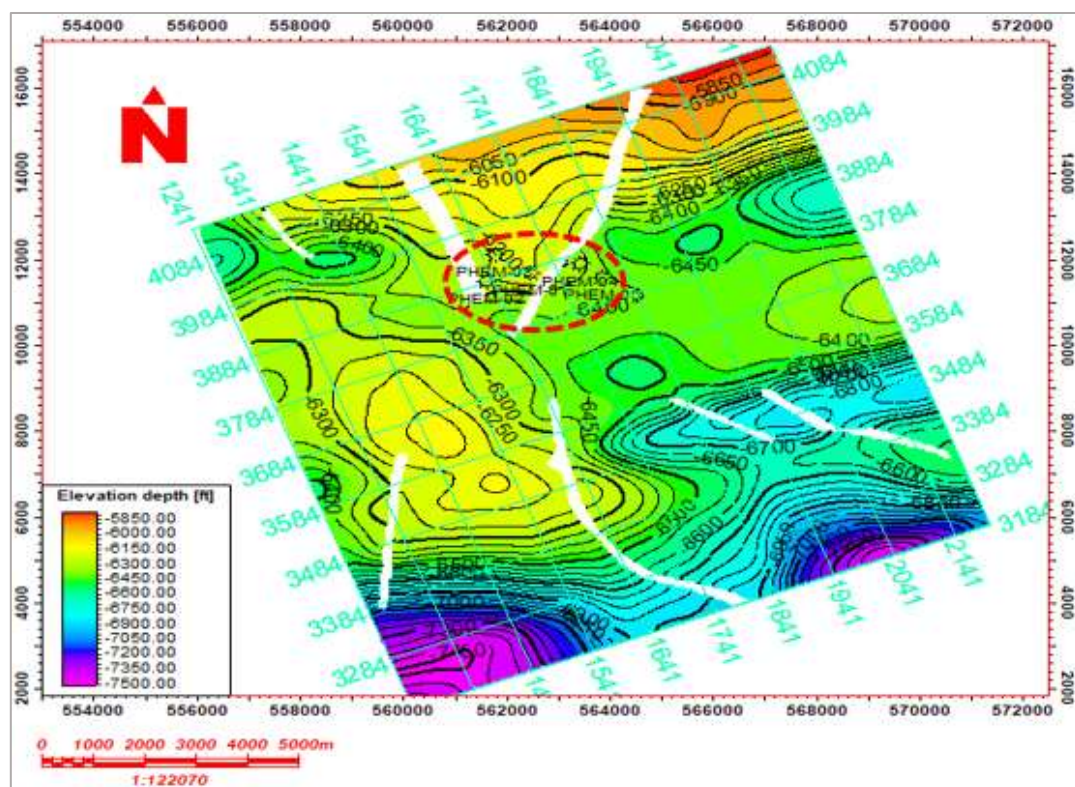


Figure 9. Depth structure map of reservoir top R-1 confirming structural highs and velocity model accuracy

4.5 Seismic attributes analysis

Seismic attributes, such as RMS amplitude and average envelope, were analyzed to enhance the identification of hydrocarbon-bearing zones. These attributes provided detailed insights into subsurface properties, aiding in more accurate geological and geophysical interpretations.

4.5.1 RMS amplitude analysis

The RMS amplitude analysis of reservoirs R-1, R-2, and R-3 offers new insights into the distribution of potential hydrocarbon-bearing zones. Figures 12, 13 and 14 illustrate the RMS amplitude maps, showing distinct patterns where high amplitudes (yellow) correspond to areas with higher sand content, indicative of favorable conditions for hydrocarbon saturation.

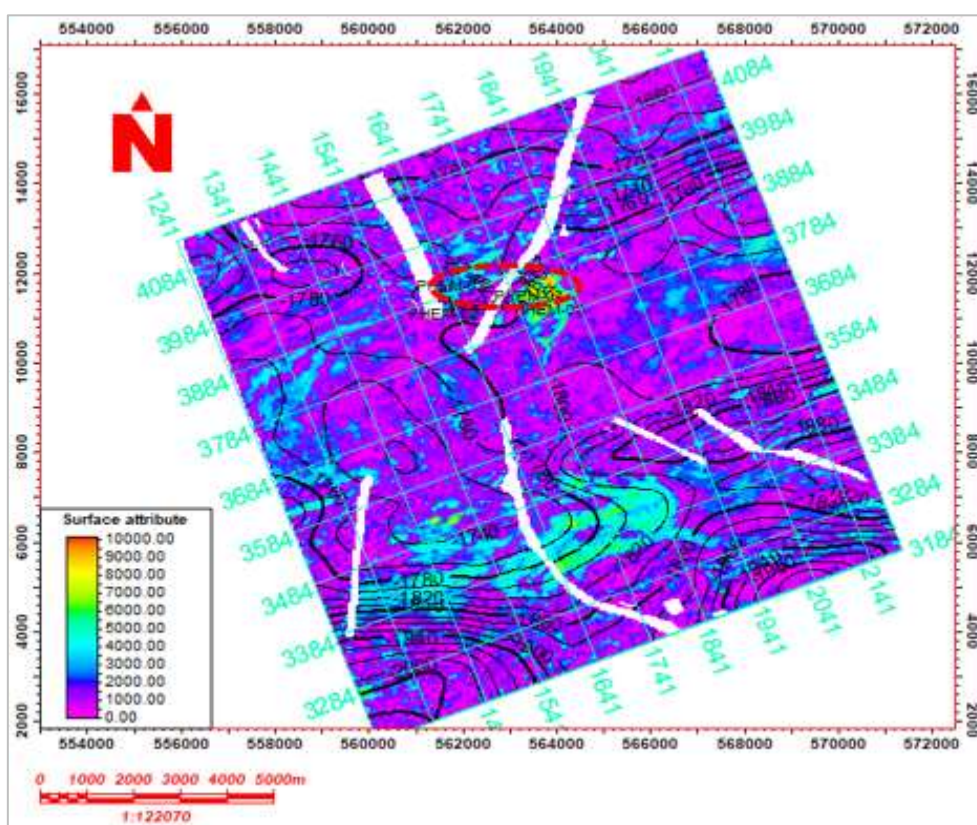


Figure 12. RMS amplitude map of reservoir top R-1 showing high-amplitude zones indicating potential high-quality reservoir sands

In contrast, low amplitudes (purple) suggest a higher shale content and less favorable reservoir characteristics. For Reservoir R-1 (Fig.12), high-amplitude zones are prominent, typically associated with high-porosity sands, suggesting the presence of high-quality reservoir facies. Similarly, Reservoir R-2 (Fig.13) features elevated amplitudes in key areas, pointing to the likelihood of high-porosity sands, which could support robust reservoir conditions. The RMS amplitude map for Reservoir R-3 (Fig.14) reveals a consistent trend, with regions of high amplitudes indicating high-porosity sands and favorable conditions for hydrocarbon-bearing facies.

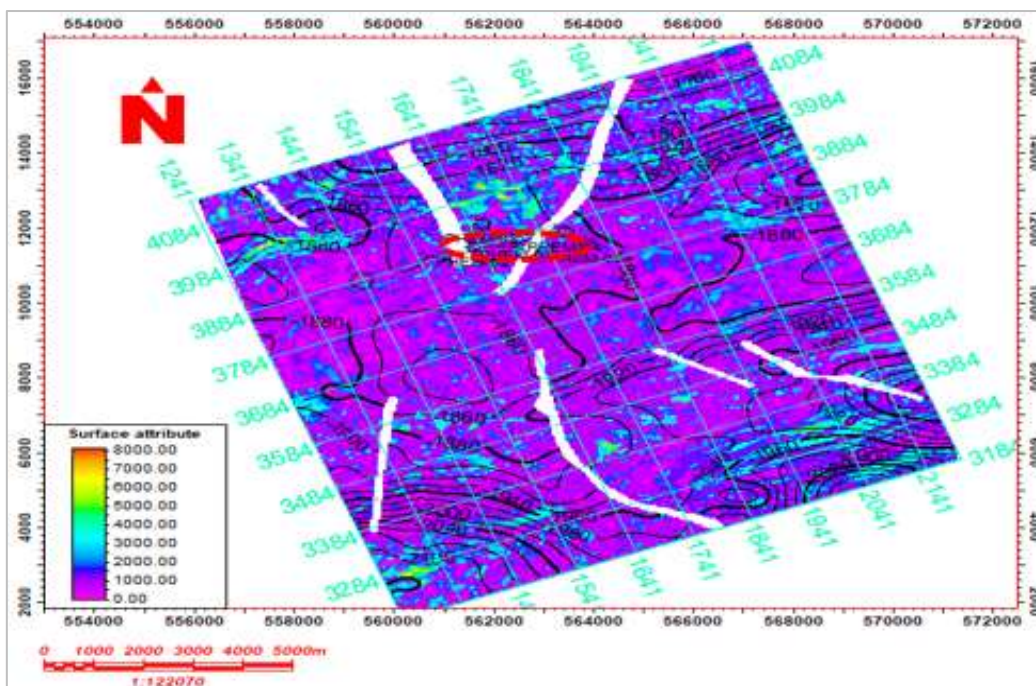


Figure 13. RMS amplitude map of reservoir top R-2 highlighting elevated amplitudes correlated with high-porosity sands

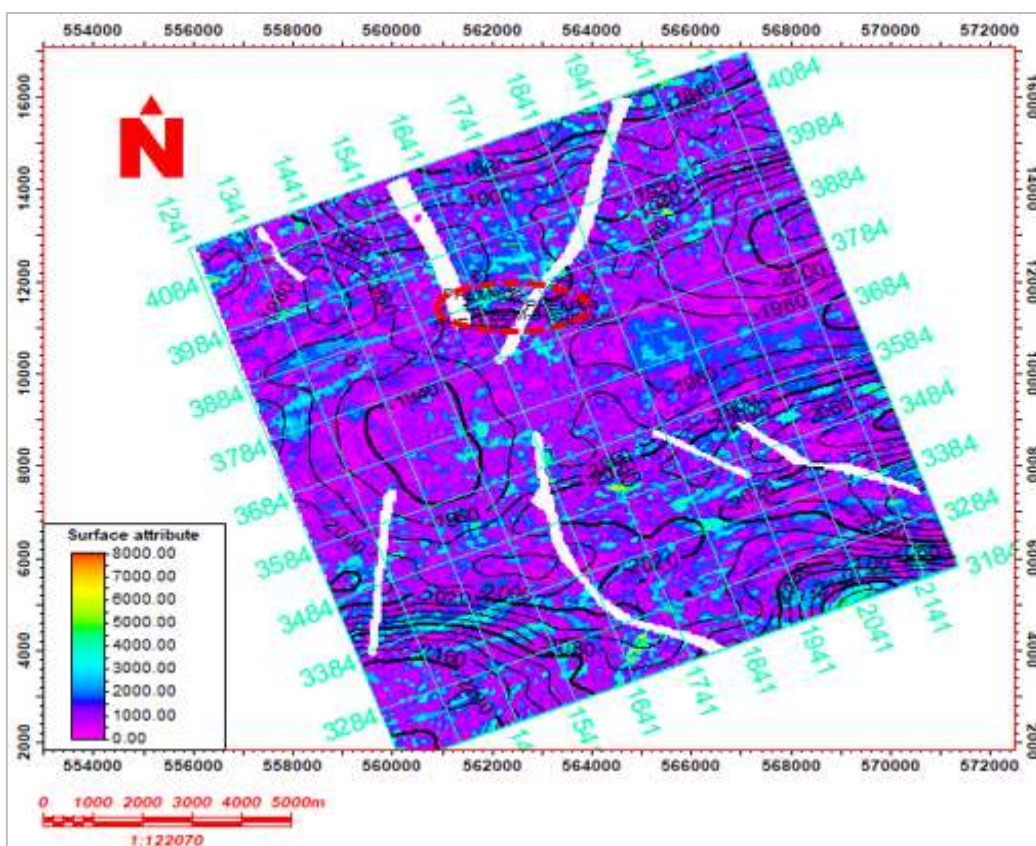


Figure 14. RMS amplitude map of reservoir top R-3 depicting strong amplitude-well correlation suggesting favorable reservoir facies

The RMS amplitude analysis across all three reservoirs emphasizes the potential of high-amplitude zones to represent high-quality, porous sands suitable for hydrocarbon accumulation, highlighting their utility for guiding exploration and optimizing well placement strategies.

4.5.2 Average envelope seismic attribute analysis

The average envelope seismic attribute analysis for reservoirs R-1, R-2, and R-3 provides new insights into the spatial distribution of favorable reservoir conditions. Figures 15, 16, and 17 display high-amplitude zones (yellow), which are associated with optimal sand-to-shale ratios and potential hydrocarbon saturation. For Reservoir R-1 (Fig.15), these elevated amplitudes indicate areas with promising reservoir facies. Similar patterns are observed in Reservoirs R-2 (Fig.16) and R-3 (Fig.17), suggesting favorable conditions for hydrocarbon accumulation. This analysis underscores the potential of high-amplitude zones as indicators of robust reservoir quality, offering strategic targets for further exploration and development.

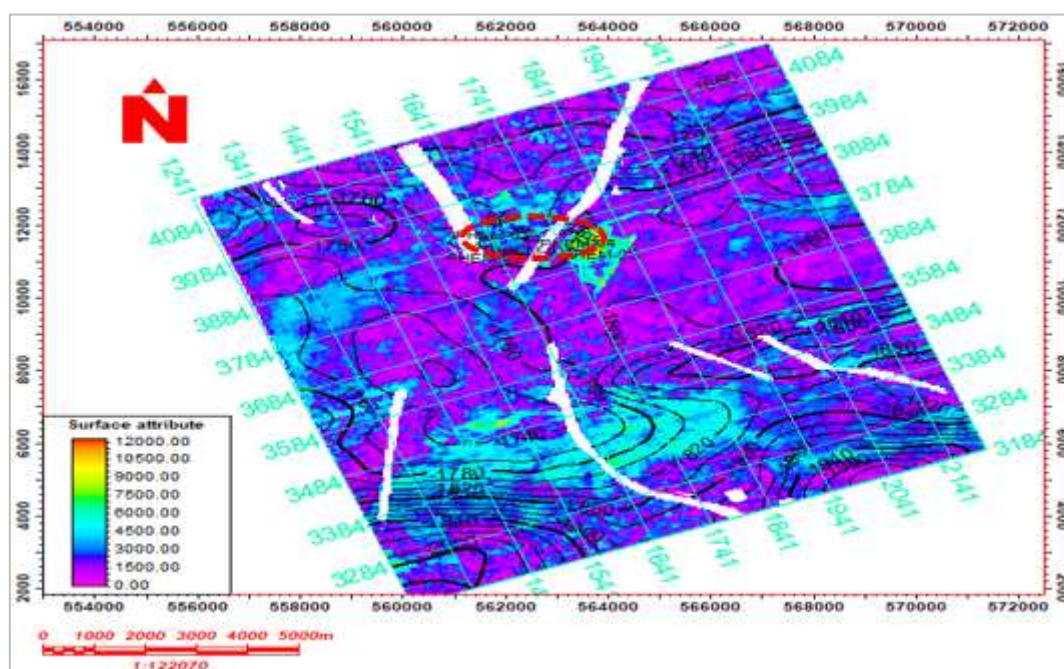


Figure 15. Average envelope attribute map of reservoir top R-1 highlighting high-amplitude zones indicating high-quality reservoir sands

4.6 Reservoir facies models

The facies modeling conducted in this study successfully delineated the lithofacies distribution, identifying sand and shale as the primary lithological units. The model (Fig.18) reveal a significant prevalence of sand across the three reservoirs, indicating strong connectivity. This widespread sand distribution suggests enhanced permeability, promoting efficient fluid flow throughout the reservoirs. These findings highlight key zones with favorable reservoir characteristics, marking them as promising targets for hydrocarbon extraction and potential future well placement.

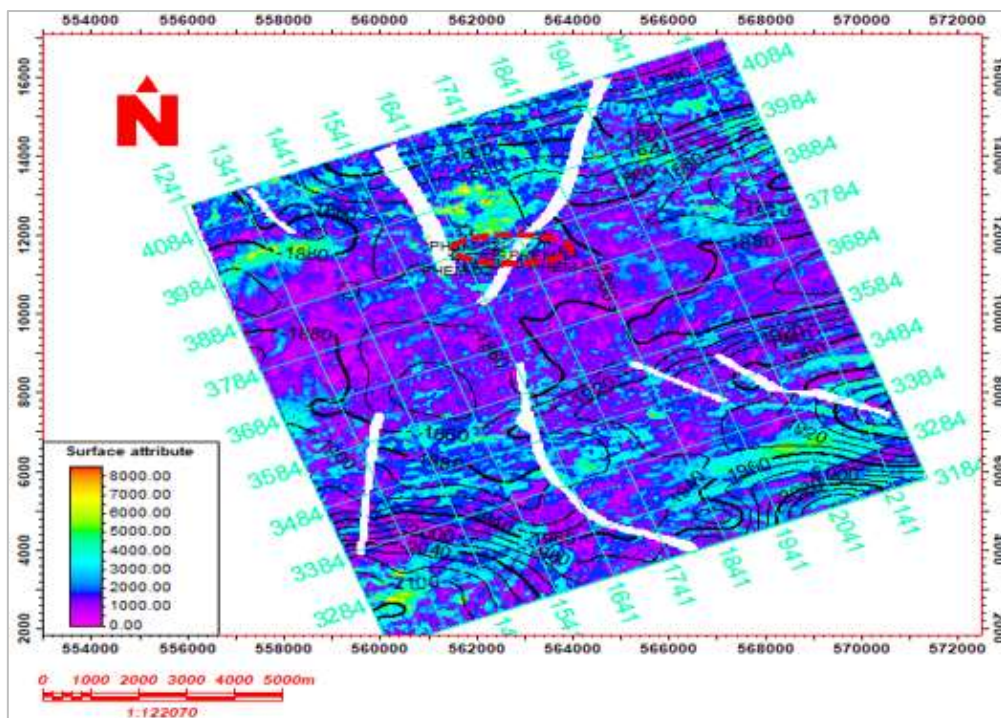


Figure 16. Average envelope attribute map of reservoir top R-2 showing strong amplitude-well alignment suggesting high-porosity sand facies

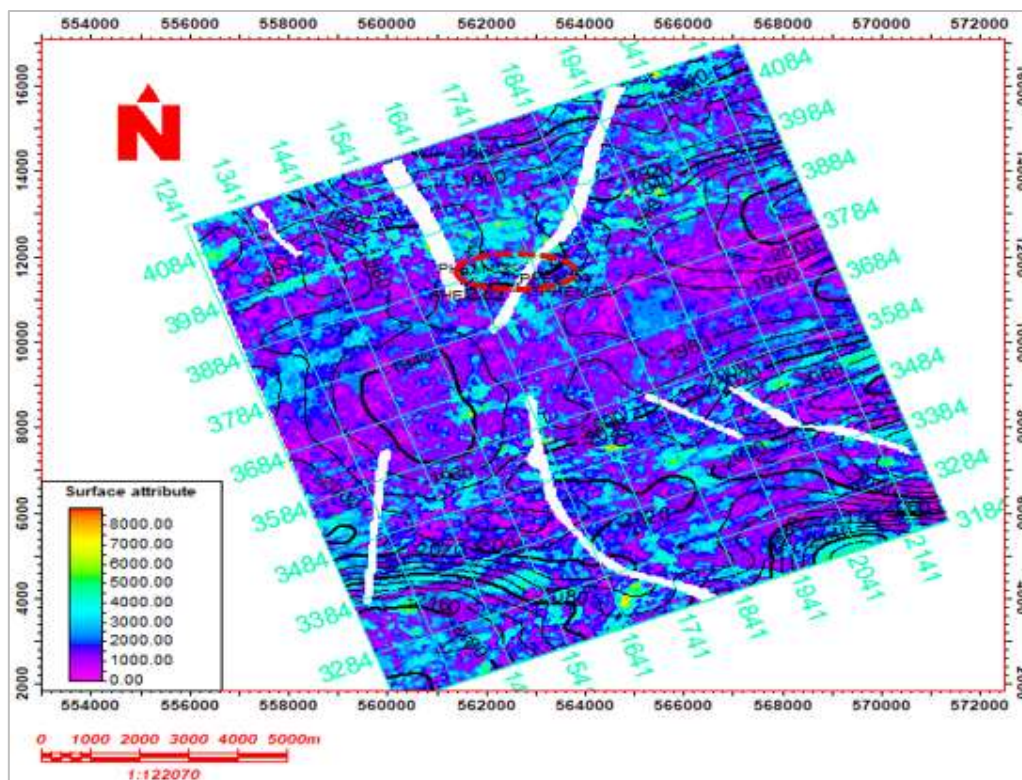


Figure 17. Average envelope attribute map of reservoir top R-3 demonstrating elevated amplitudes correlated with quality reservoir prospects

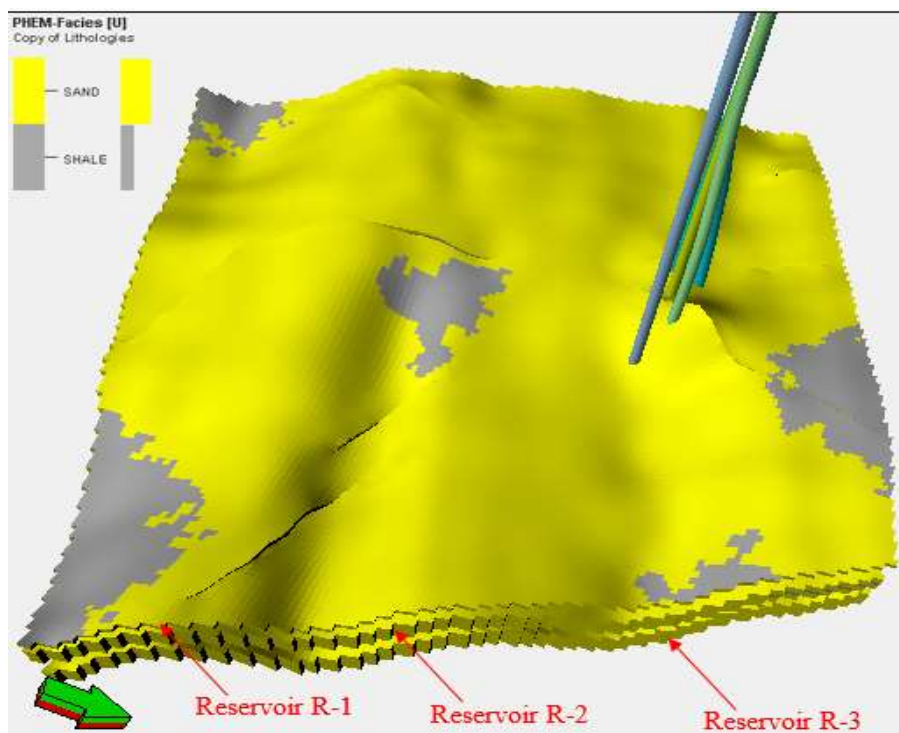


Figure 18. Lithofacies model showing distribution of sand and shale units across the three reservoirs, indicating high sand connectivity and strategic well placement

4.7 Petrophysical modelling results

The petrophysical models for reservoirs R-1, R-2, and R-3 highlight the distribution of reservoir properties. Utilizing the Sequential Gaussian Simulation (SGS) method, these models effectively capture the spatial variability of key petrophysical parameters within a 3-D grid.

4.7.1 Net-to-gross thickness model results

The net-to-gross (NTG) thickness model developed for the study area highlights the distribution of sand across the three reservoirs. Figure 19 shows that the NTG values range from 55% to 95%, indicating sand coverage from fair to very good across the field. This variation reflects differing levels of sand distribution within the reservoirs. The analysis identifies regions with NTG values between 80% and 90% as having higher sand presence, suggesting areas of superior reservoir quality. These findings underscore the value of NTG analysis in assessing reservoir heterogeneity, aiding in identifying zones with the potential for efficient hydrocarbon production and guiding future well placement strategies.

4.7.2 Porosity model results

The porosity models for reservoirs R-1, R-2, and R-3 highlight key characteristics of pore structure and reservoir quality. Figure 20 illustrates total porosity distribution ranging from 0.12 to 0.42, indicating fair to excellent porosity levels and suggesting variations in hydrocarbon storage capacity. Effective porosity, shown in Figure 21, ranges from 0.07 to 0.35, slightly lower than total porosity due to shale content.

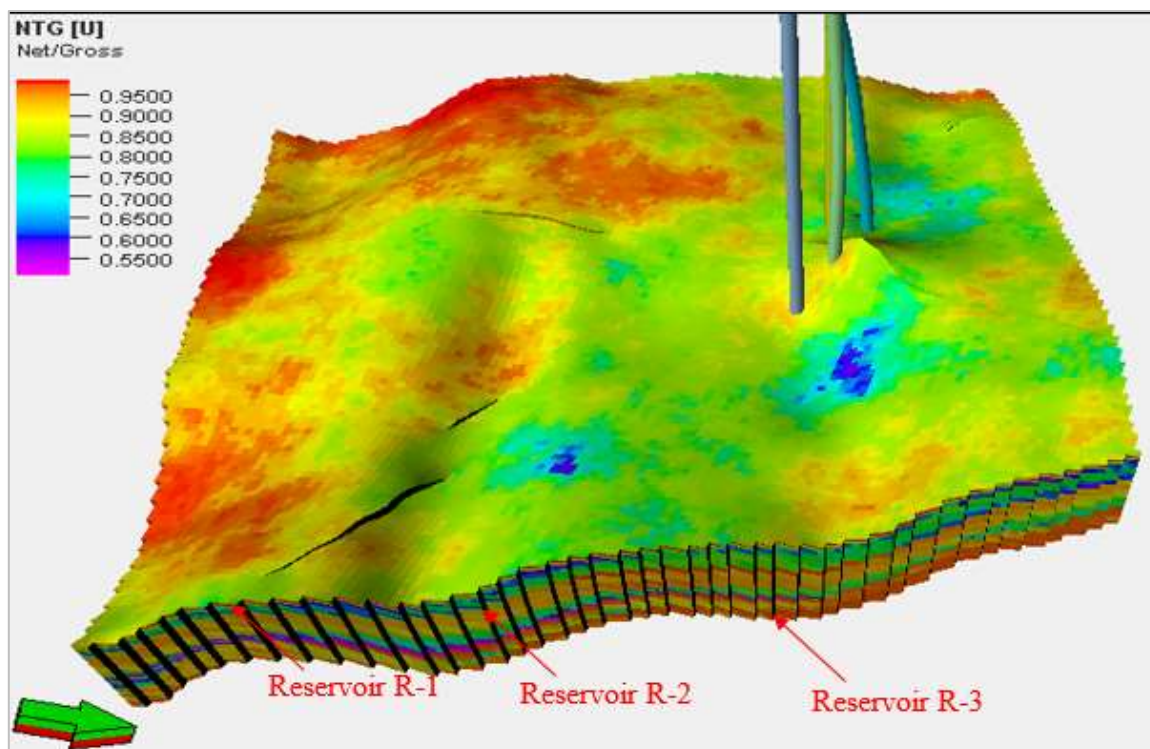


Figure 19. Net-to-gross thickness model showing sand distribution and variability across reservoirs R-1, R-2, and R-3, with study well locations

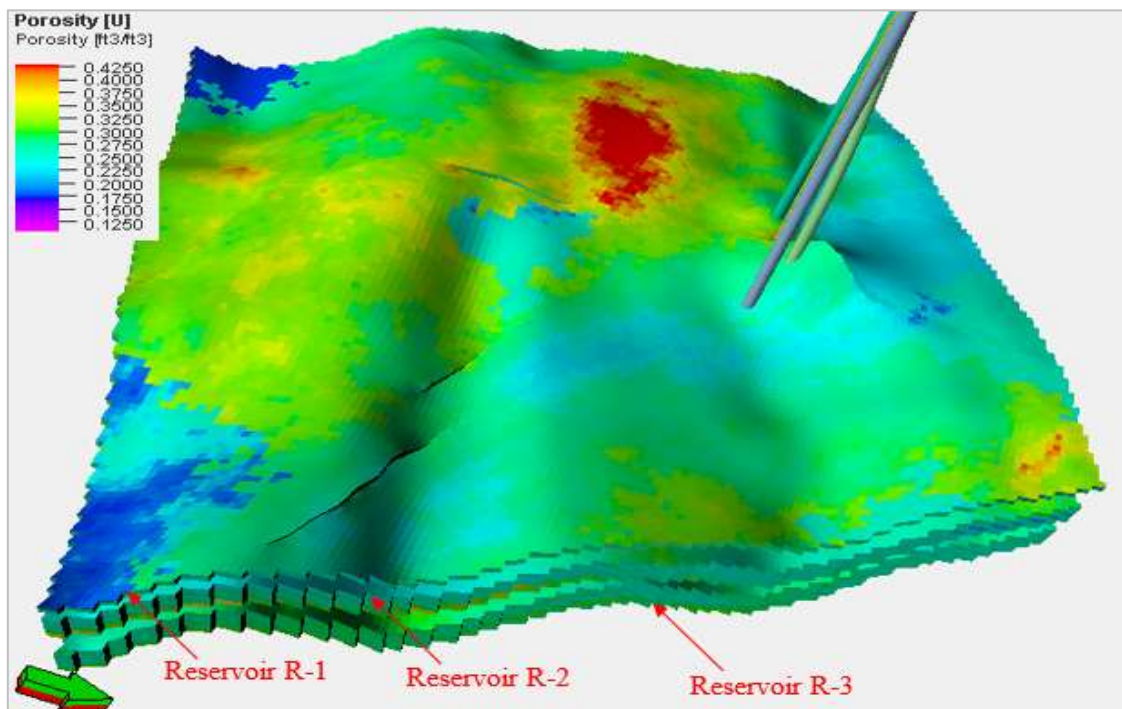


Figure 20. Total porosity model for reservoirs R-1, R-2, and R-3 showing variability in porosity ranging from fair to excellent across the study area

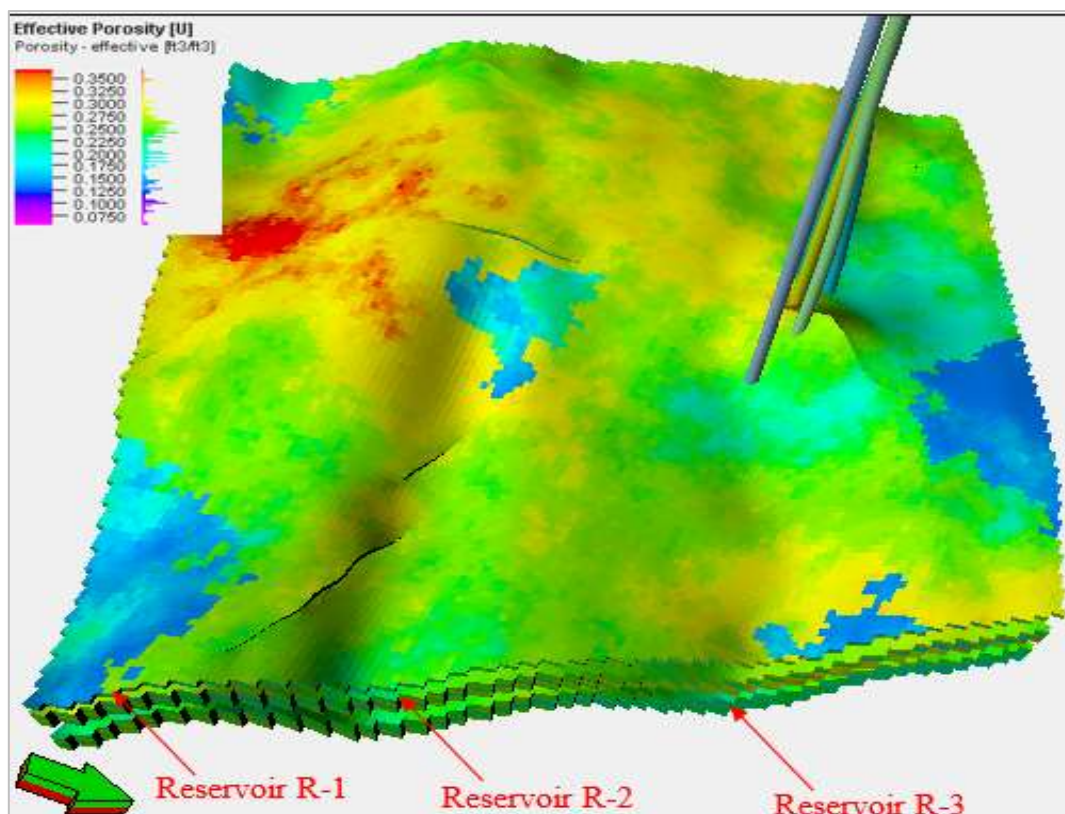


Figure 21. Effective porosity model for reservoirs R-1, R-2, and R-3 indicating distribution of interconnected pore spaces with fair to very good connectivity

This model captures the volume of interconnected pore spaces, essential for fluid flow and reservoir performance. These findings underscore the importance of both total and effective porosity in evaluating reservoir quality, pinpointing zones with strong pore connectivity, and supporting efficient hydrocarbon production and strategic well placement.

4.7.3 Permeability model results

The permeability models for reservoirs R-1, R-2, and R-3 highlight fluid flow potential across the study area. Figure 22 displays permeability values ranging from 10 to 1,000 millidarcy, reflecting varying reservoir quality. High-permeability zones indicate enhanced pore connectivity, essential for efficient hydrocarbon flow and accumulation. These findings emphasize the significance of identifying areas with superior permeability, offering valuable guidance for optimizing hydrocarbon recovery and future well placement strategies.

4.7.4 Water saturation model results

The water saturation model for reservoirs R-1, R-2, and R-3, as shown in Figure 23, displays saturation values from 0 to 1, indicating variable water content across the reservoirs. Areas of low water saturation point to zones of high hydrocarbon presence, which are favorable for production. These results highlight key targets with low water saturation, enhancing the potential for efficient hydrocarbon recovery and guiding future well placement.

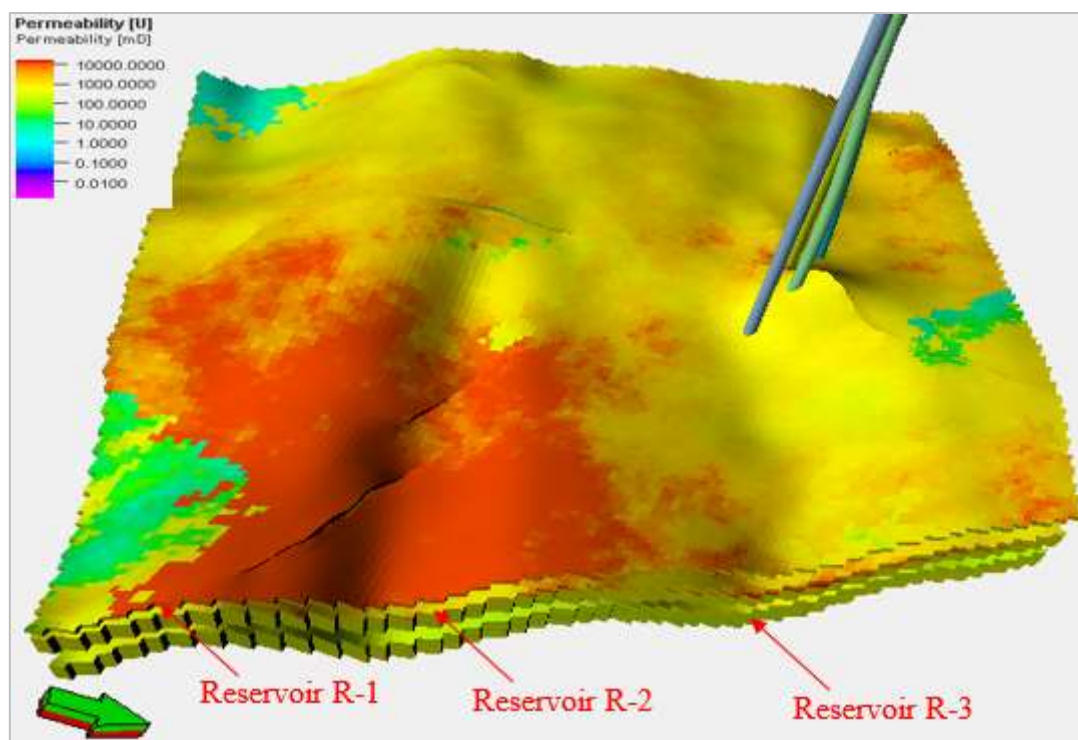


Figure 22. Permeability model for reservoirs R-1, R-2, and R-3 showing variability in permeability ranging from 10 – 1000 mD across the study area

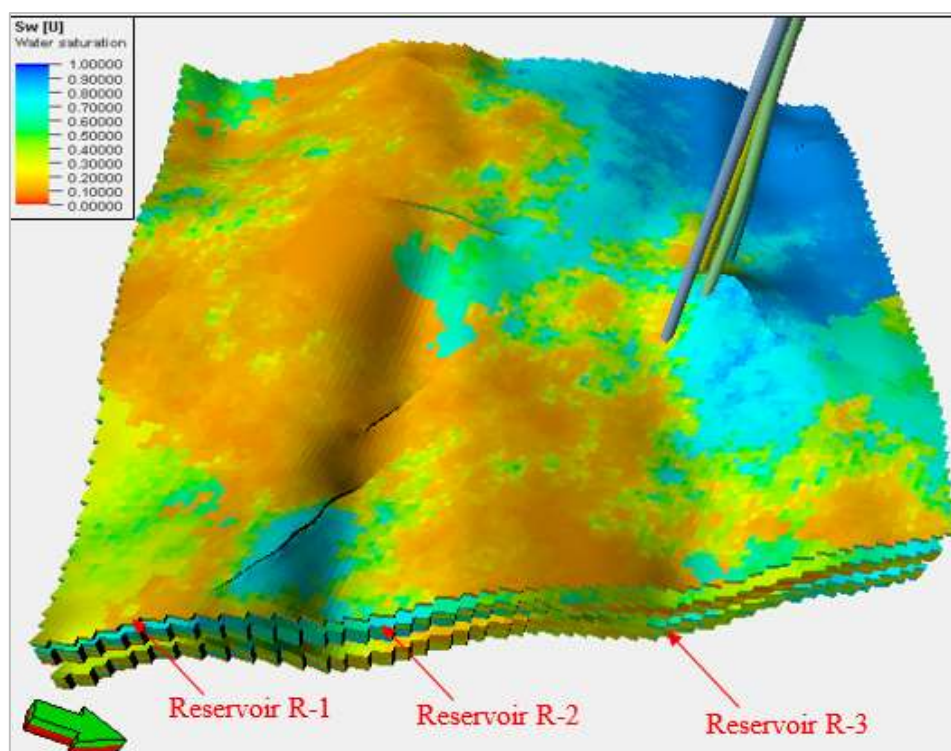


Figure 23. Water saturation model for reservoirs R-1, R-2, and R-3 showing variability in water saturation values from 0 to 1, with study well locations in low saturation regions

4.7.5 Hydrocarbon saturation model results

The hydrocarbon saturation model for reservoirs R-1, R-2, and R-3, shown in Figure 24, highlights hydrocarbon distribution with saturation values ranging from 0.1 to 0.9. This range indicates a strong hydrocarbon presence throughout the formations, suggesting substantial extraction potential. Areas with elevated hydrocarbon saturation mark promising zones for future development, supporting effective hydrocarbon recovery. These findings underscore the reservoirs' productive capacity, reinforcing their significance for exploration and extraction initiatives.

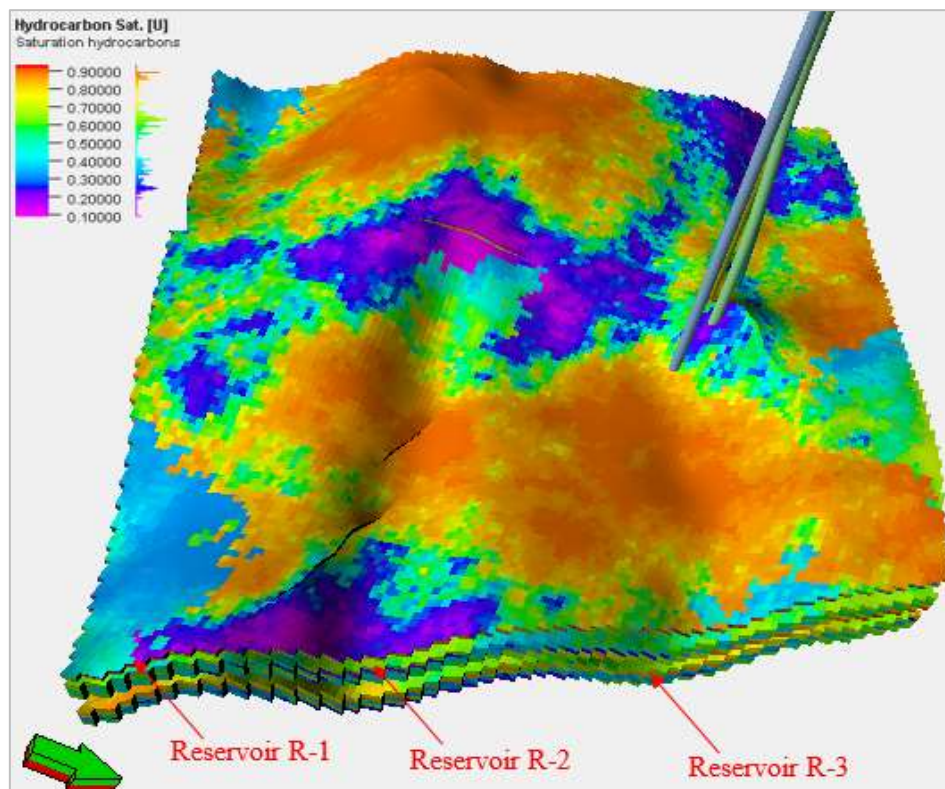


Figure 24. Hydrocarbon saturation model for reservoirs R-1, R-2, and R-3 showing hydrocarbon saturation values ranging from 0.1 – 0.9, with study well locations indicating high hydrocarbon potential

5 CONCLUSION

The research presents a comprehensive reservoir characterization of the Phem Field, offshore Niger Delta, by integrating seismic attributes and reservoir property modeling. This study's novel approach, incorporating detailed seismic attribute analysis alongside robust petrophysical and facies modeling, offers a more accurate and insightful understanding of reservoir properties and hydrocarbon distribution within the field. Key findings highlight the advantages of using seismic and petrophysical models in understanding lithology, structure, and fluid distribution, leading to enhanced reservoir quality assessment and optimized well placement. By implementing attributes like RMS amplitude and average envelope analysis, the study effectively delineates high-amplitude zones that correlate with sand-rich, hydrocarbon-bearing facies. The petrophysical models, including NTG, porosity, permeability, and hydrocarbon saturation, further illustrate the spatial distribution of essential reservoir parameters, offering insights into reservoir heterogeneity and the connectivity of hydrocarbon-bearing sands. These models demonstrate potential hydrocarbon-rich zones and highlight favorable regions for future exploration and drilling strategies. The successful integration of seismic and petrophysical data in this study sets a foundation for advanced reservoir modeling techniques in similar fields, providing a framework for hydrocarbon exploration and production.

Highlights:

- Enhanced seismic attribute analysis reveals high-amplitude zones, highlighting sand-rich, hydrocarbon-bearing facies.
- Petrophysical models (NTG, porosity, permeability, hydrocarbon saturation) illustrate reservoir heterogeneity and aid in identifying hydrocarbon-rich zones.
- Facies models indicate significant sand connectivity, suggesting high permeability and efficient fluid flow potential.
- Depth and time structure maps confirm the robustness of the velocity model, supporting reliable hydrocarbon trapping mechanisms.
- Integrated seismic and petrophysical modeling improves accuracy in reservoir quality assessment, optimizing hydrocarbon extraction strategies.

This integration serves as a valuable approach for future reservoir studies in offshore Niger Delta and other analogous hydrocarbon-bearing regions.

ACKNOWLEDGMENTS

I extend my sincere thanks to the research team at the Department of Applied Geophysics, Olusegun Agagu University of Science and Technology, Ondo State, Nigeria, for providing the essential facilities that greatly contributed to this investigation.

REFERENCES

- [1] ARCHIE, G.E. The electrical resistivity log as an aid in determining some reservoir characteristics. *Transactions of the AIME*. 1942, vol. 146, no. 01, pp. 54–62. Available from: <https://doi.org/10.2118/942054-G>.
- [2] ARCHIE, G.E. Introduction to petrophysics of reservoir rocks. *AAPG Bulletin*. 1950, vol. 34, no. 5, pp. 943–961.
- [3] ASQUITH, G.; KRYGOWSKI, D.; HENDERSON, S. and HURLEY, N. (ed.). *Basic Well Log Analysis*. Tulsa, Oklahoma: The American Association of Petroleum Geologists, 2004. ISBN 0891816674. Available from: <https://doi.org/10.1306/Mth16823>.
- [4] BAKER, R.; PRINGLE, J. and SMITH, R. *Reservoir Modelling: A Practical Guide*. Wiley, 2010. Available from: <https://doi.org/10.1002/9781119313458.ch1>.
- [5] BARNES, A.E. *Handbook of Poststack Seismic Attributes*. Society of Exploration Geophysicists, 2007. Available from: <https://doi.org/10.1190/1.9781560803324>.
- [6] BROWN, A.R. *Interpretation of Three-Dimensional Seismic Data*. AAPG Memoir 42, 2004. Available from: <https://doi.org/10.1306/M4271346>.
- [7] CHEN, Q. and SIDNEY, S. Seismic attribute technology for reservoir forecasting and monitoring. *The Leading Edge*. 1997, vol. 16, no. 5, pp. 445–456. Available from: <https://doi.org/10.1190/1.1437657>.
- [8] CHOPRA, S. and MARFURT, K.J. Seismic Attributes – a promising aid for geologic prediction. *CSEG Recorder*. 2005, vol. 30, no. 1, 18–33. Available from: <https://api.semanticscholar.org/CorpusID:16131008>.
- [9] CHOPRA, S. and MARFURT, K.J. *Seismic Attributes for Prospect Identification and Reservoir Characterization*. Society of Exploration Geophysicists, 2007. Available from: <https://doi.org/10.1190/1.9781560801900>.
- [10] DAKE, L.P. *Fundamentals of Reservoir Engineering*. Elsevier, 2001. Available from: <https://api.semanticscholar.org/CorpusID:92911934>.

- [11] DOUST, H. and OMATSOLA, E.M. Niger Delta. In: *Divergent/Passive Margins Basins.*, American Association of Petroleum Geologists, 1990, pp. 239–248. Available from: <https://doi.org/10.1306/M48508C4>.
- [12] DOYEN, P.M. *Seismic Reservoir Characterization: An Earth Modelling Perspective*. EAGE, 2007. Available from: <http://dx.doi.org/10.3997/9789073781771>.
- [13] DUBRULE, O. *Geostatistics for Seismic Data Integration in Earth Models*. Society of Exploration Geophysicists, 2003. Available from: <https://doi.org/10.1190/1.9781560801962>.
- [14] EJEDAWE, J.E.; COKER, S.J.L.; LAMBERT-AIKHIONBARE, D.O.; ALOFE, K.B. and ADOH, F.O. Evolution of oil-generative window and oil and gas occurrence in Tertiary Niger Delta Basin. *AAPG Bulletin*. 1984, vol. 68, pp. 1744–1751. Available from: <https://doi.org/10.1306/AD46198F-16F7-11D7-8645000102C1865D>.
- [15] HALDORSEN, H.H. and DAMSLETH, E. Stochastic modeling. *Journal of Petroleum Technology*. 1990, vol. 42, no. 4, pp. 404–412. Available from: <https://api.semanticscholar.org/CorpusID:109342947>.
- [16] HIRSCH, K.H.; LUCAS, K.J. and WONG, J.C. Pitfalls and limitations in seismic attribute analysis. *The Leading Edge*. 1998, vol. 17, no. 2, pp. 145–148.
- [17] HOSPERS, J. Gravity Field and Structure of the Niger Delta, Nigeria, West Africa. *Geological Society of America Bulletin*. 1965, vol. 76, no. 4, pp. 407–422. Available from: [https://doi.org/10.1130/0016-7606\(1965\)76\[407:GFASOT\]2.0.CO;2](https://doi.org/10.1130/0016-7606(1965)76[407:GFASOT]2.0.CO;2).
- [18] HUNT, J.M. Generation and migration of petroleum from abnormally pressured fluid compartments. *AAPG Bulletin*. 1990, vol. 74, pp. 1–12. Available from: <https://doi.org/10.1306/0C9B21EB-1710-11D7-8645000102C1865D>.
- [19] KAPLAN, A.; LUSSEY, C.U. and NORTON, I.O. *Tectonic Map of the World, Panel 10*. 1:10,000,000. Tulsa: American Association of Petroleum Geologists, 1994
- [20] KLETT, T.R.; AHLBRANDT, T.S.; SCHMOKER, J.W. and DOLTON, J.L., 1997. *Ranking of the world's oil and gas provinces by known petroleum volumes*. CD-ROM. USGS Open-file Report 97–463. U. S. Department of the Interior, Geological Survey, 1997. Available from: <https://doi.org/10.3133/ofr97463>.
- [21] KULKE, H., 1995. *Regional Petroleum Geology of the World. Part II: Africa, America, Australia, and Antarctica*. Berlin: Gebrüder Borntraeger, 1995.
- [22] LAKE, L.W.; JOHNS, R.T.; ROSSEN, W.R. and POPE, G.A. *Fundamentals of Enhanced Oil Recovery*. Society of Petroleum Engineers, 2014. Available from: <https://doi.org/10.2118/9781613993286>.
- [23] LEHNER, P. and De RUITER, P.A.C., 1977. Structural history of Atlantic Margin of Africa. *AAPG Bulletin*. 1977, vol. 61, pp. 961–981. Available from: <https://doi.org/10.1306/C1EA43B0-16C9-11D7-8645000102C1865D>.
- [24] MA, X. Seismic attributes in reservoir characterization: Methodologies and applications. *Interpretation*. 2011, vol. 1, no. 2, pp. 1–12.
- [25] MA, Y.; ZHANG, H.; LIU, J. and ZHAO, X. Application of integrated geophysics for reservoir characterization. *Journal of Applied Geophysics*. 2011, vol. 75, no. 4, pp. 507–516.
- [26] MAUCEC, M.; DOBROVA, E. and VESELINOVIC, J. *Reservoir Characterization and Modeling: A Geostatistical Approach*. Elsevier, 2013.
- [27] MIALL, A.D. *Principles of Sedimentary Basin Analysis*. Springer, 2010. Available from: http://dx.doi.org/10.1007/978-3-662-03999-1_2.
- [28] MU, L.; MARFURT, K.J. and LIU, J. Multiattribute seismic analysis to delineate channels and their fills: A case study of the Barnett Shale, Fort Worth Basin, Texas. *Geophysics*. 2008, vol. 73, no. 2, pp. B23–B30.
- [29] NELSON, P.H. Permeability-porosity relationships in sedimentary rocks. *The Log Analyst*. 1994, vol. 35, no. 3, pp. 38–62.
- [30] NTON, M.E. and SALAMI, R. Reservoir characteristics and palaeo-depositional environment of Duski Field, onshore, Niger Delta, Nigeria. *Global Journal of Geological Sciences*. 2016, vol. 14, pp. 49–63. Available from: <http://dx.doi.org/10.4314/gjgs.v14i1.5>.
- [31] OLADELE, S.; SALAMI, R. and ADEYEMI, O. Petrophysical and rock physics analyses for characterization of complex sands in deepwater Niger Delta, Nigeria. *GeoScience Engineering*. 2019, vol. 65, no. 2, pp. 24–35. Available from: <https://doi.org/10.35180/gse-2019-0009>.
- [32] OLADELE, S.; SALAMI, R. and ONAYEMI, J. Rock physics modelling of sub-seismic reservoirs in complex depositional systems: Case study of sand K2, Kuti Field, deepwater Niger Delta, Nigeria. *Technical Journal, University of Engineering and Technology (UET) Taxila*. 2023, vol. 28, no. 2, pp. 1–8. ISSN:1813-1786. Available from: <https://tj.uettaxila.edu.pk/index.php/technical-journal/article/view/1670>.

- [33] OLADELE, S.; SALAMI, R.; ONAYEMI, J. and FOLARIN, O. Electrofacies characterization of sequence in Ray Field, Niger Delta, Nigeria. *FUW Trends in Science and Technology Journal*. 2020, vol. 5, no. 2, pp. 430–436. Available from: www.ftstjournal.com.
- [34] PYRCZ, M.J. and DEUTSCH, C.V. *Geostatistical Reservoir Modeling*. Oxford University Press, 2014.
- [35] SALAMI, R. and OMONIJO, O.E. Reservoir characterization using artificial neural network in X field, Niger Delta, Nigeria. *Coast Journal of School Science*. 2022, vol. 4, no. 1, pp. 731–742.
- [36] SCHLUMBERGER. *Log Interpretation Principles/Applications*. Schlumberger Educational Services, 1989.
- [37] SCHLUMBERGER. *Petrel E&P Software Platform*, 2017.
- [38] SCHLUMBERGER. *Well Logging and Formation Evaluation*. Retrieved from Schlumberger Oilfield Glossary, 2024.
- [39] SCHWAB, A.; NICHOLS, J. and JOHNSTON, D. Advanced seismic inversion techniques for enhanced reservoir characterization. *First Break*. 2011, vol. 29, no. 5, pp. 61–69.
- [40] SHERIFF, R.E. and GELDART, L.P. *Exploration Seismology*. Cambridge University Press, 1995. ISBN 9781139168359. Available from: <https://doi.org/10.1017/CBO9781139168359>.
- [41] Well Log Interpretation. In: *SPE E&P Glossary*. Society of Petroleum Engineers (SPE). (2024).
- [42] TANER, M. T.; KOEHLER, F. and SHERIFF, R.E. Complex seismic trace analysis. *Geophysics*. 1979, vol. 44, no. 6, pp. 1041–1063. Available from: <https://doi.org/10.1190/1.1440994>.
- [43] TIAB, D. and DONALDSON, E.C. *Petrophysics: Theory and Practice of Measuring Reservoir Rock and Fluid Transport Properties*. Gulf Professional Publishing, 2012.
- [44] WORTHINGTON, P.F. *The Evolution of Petrophysics*. Petroleum Exploration Society of Great Britain, 2011.
- [45] YILMAZ, O. *Seismic Data Analysis: Processing, Inversion, and Interpretation of Seismic Data*. Society of Exploration Geophysicists, 2001. Available from: <https://doi.org/10.1190/1.9781560801580>